

## Growth and Transport Properties of (110)-Oriented $\text{La}_{2/3}\text{Sr}_{1/3}\text{MnO}_3$ Thin Films on $\text{TiO}_2$ -Buffered Si (100) Substrates

This content has been downloaded from IOPscience. Please scroll down to see the full text.

2003 Jpn. J. Appl. Phys. 42 L287

(<http://iopscience.iop.org/1347-4065/42/3B/L287>)

View [the table of contents for this issue](#), or go to the [journal homepage](#) for more

Download details:

IP Address: 140.113.38.11

This content was downloaded on 28/04/2014 at 03:15

Please note that [terms and conditions apply](#).

## Growth and Transport Properties of (110)-Oriented $\text{La}_{2/3}\text{Sr}_{1/3}\text{MnO}_3$ Thin Films on $\text{TiO}_2$ -Buffered Si (100) Substrates

Shiu-Jen LIU\*, Shyh-Feng CHEN, Jenh-Yih JUANG, Jiunn-Yuan LIN<sup>1</sup>, Kaung-Hsiung WU, Tseng-Ming UEN and Yi-Shun GOU

Department of Electrophysics, National Chiao Tung University, Hsinchu, Taiwan 300, R.O.C.

<sup>1</sup>Institution of Physics, National Chiao Tung University, Hsinchu, Taiwan 300, R.O.C.

(Received October 10, 2002; revised manuscript received January 14, 2003; accepted for publication January 20, 2003)

The growth and transport properties of (110)-oriented  $\text{La}_{2/3}\text{Sr}_{1/3}\text{MnO}_3$  thin films on  $\text{TiO}_2$ -buffered silicon substrates by pulsed-laser deposition are reported. An insulator-metal transition associated with a ferromagnetic transition was observed at about 360 K. Magnetic measurements showed that in-plane coercive fields are about 60 Oe and 300 Oe at 300 K and 5 K, respectively. A magnetoresistance with a  $\Delta\rho/\rho(H=0)$  ratio of  $-20\%$  in a magnetic field of 5 T was observed not only near the insulator-metal transition temperature but also below 30 K. Moreover, a  $T^2$ - to  $T^3$ -dependence crossover of resistivity was observed around 60 K, indicating that an unconventional one-magnon scattering may have occurred.  
[DOI: 10.1143/JJAP.42.L287]

KEYWORDS: colossal magnetoresistance, buffer layer, hole-doped manganite, titanium dioxide, transport properties, pulsed-laser deposition, one-magnon scattering, insulator-metal transition

Hole-doped rare-earth manganites  $\text{Ln}_{1-x}\text{A}_x\text{MnO}_3$ , where Ln and A are trivalent lanthanide and divalent alkaline-earth ions, respectively, have attracted much attention because of their unusual magnetic and electronic properties. The colossal magnetoresistance (CMR) observed near the insulator-metal transition temperature ( $T_{\text{IM}}$ ) is one of the most important characteristics of these materials. Extensive studies revealed that the optimally doped La–Sr–Mn–O (LSMO) is half-metallic.<sup>1,2)</sup> That is, charge carriers responsible for the metallic behavior have the same spin, whereas carriers with the opposite spin are insulating. The half-metallic nature of the manganite materials exhibiting CMR characteristics has made them a candidate for spin-dependent electronic devices, which are expected to play a key role in the next-generation electronic industry.<sup>3,4)</sup>

From the application point of view, growing CMR films on technologically viable substrates is of vital importance. Several groups have attempted to grow manganite films on Si, the most prominent material used in semiconducting devices. However, the manganite films directly grown on Si were mainly (110) textured but mixed with many other orientations.<sup>5,6)</sup> To improve the epitaxy of manganite films on Si, several buffer layers have been introduced, such as yttria-stabilized  $\text{ZrO}_2$  (YSZ),<sup>7)</sup>  $\text{Si}_3\text{N}_4$ ,<sup>8)</sup>  $\text{SrTiO}_3/\text{TiN}$ <sup>9)</sup> and  $\text{SrTiO}_3/\text{MgO}/\text{TiN}$ .<sup>10)</sup> The results indicated that La–Ca–Mn–O (LCMO) films can be epitaxially grown on buffered Si. However, the  $T_{\text{IM}}$  of these films and, hence, the temperature of the maximum magnetoresistance (MR) were reduced significantly. The attempt of using  $\text{CeO}_2$ -buffered Si for growing LCMO films has resulted in crystalline structures similar to the ones directly grown on Si.<sup>11)</sup> Perhaps one of the best results along this line was that demonstrated by Trajanovic *et al.*<sup>12)</sup> who used a multi layered buffer consisting of YSZ and  $\text{Bi}_4\text{Ti}_3\text{O}_{12}$ .

$\text{TiO}_2$  is one of the most extensively studied transition-metal oxides. The preparation of  $\text{TiO}_2$  thin films has received much attention during the last decade because of their remarkable optical and electronic properties. It is known that  $\text{TiO}_2$  exists in three different crystalline phases:

anatase and rutile (both tetragonal), and brookite (orthorhombic). Only anatase and rutile have been observed in thin films up to now. Recently, it was found that high- $T_{\text{C}}$  superconducting  $\text{YBa}_2\text{Cu}_3\text{O}_{7-y}$  films can be grown on  $\text{TiO}_2$  rutile epitaxially.<sup>14)</sup> In this article, we report the *in situ* deposition of pure (110)-oriented LSMO thin films on Si (100) substrates by using a  $\text{TiO}_2$  rutile buffer layer. The  $T_{\text{IM}}$  and ferromagnetic Curie temperature ( $T_{\text{C}}$ ) of the as-grown films, in contrast to the previous results, remain very close to the reported bulk values. Moreover, the half-metallic nature of these films is clearly demonstrated.

The  $\text{TiO}_2$  rutile buffer layer was deposited by similar procedures used for obtaining epitaxial  $\text{CrO}_2$  films on buffered Si substrates.<sup>13)</sup> Briefly, the TiN layer was deposited by pulsed-laser deposition (PLD) on the Si (100) substrate at  $650^\circ\text{C}$  with a laser energy density of  $4\text{J}/\text{cm}^2$ . The PLD chamber was maintained under a base pressure of  $4 \times 10^{-5}$  Torr during the deposition. When the deposition of TiN was completed, the substrate temperature was raised to  $750^\circ\text{C}$  and the chamber was filled with pure oxygen up to 0.4 Torr. After maintaining these conditions for 10 min, the TiN layer was converted into  $\text{TiO}_2$  rutile,<sup>14)</sup> and the LSMO film was then deposited *in situ* on the  $\text{TiO}_2$ -buffered Si substrate. Upon completing the deposition of the LSMO film, the chamber was filled with 700 Torr  $\text{O}_2$  and the substrate was cooled to room temperature at a rate of  $15^\circ\text{C}/\text{min}$ . The thickness of both of the  $\text{TiO}_2$  layer and LSMO film was about 50 nm. The lattice structure and surface morphology of as-grown films were examined by X-ray diffraction (XRD) scans and scanning tunneling microscopic (STM) measurements, respectively. The resistivity and magnetization measurements were carried out using a quantum design physical property measurement system (PPMS). All MR and magnetization measurements in this work were performed with the application of magnetic field along the surface of the films.

Figure 1 shows the typical  $\theta$ - $2\theta$  XRD pattern of the LSMO/ $\text{TiO}_2$ /Si multi layer structure. Except for the peaks of the  $\text{TiO}_2$  buffer layer and Si substrate, only the (110) peaks of LSMO were observed. The XRD scans indicate that the  $\text{TiO}_2$  buffer layer and the LSMO film are both purely (110)-

\*E-mail address: sjliu.ep86g@nctu.edu.tw

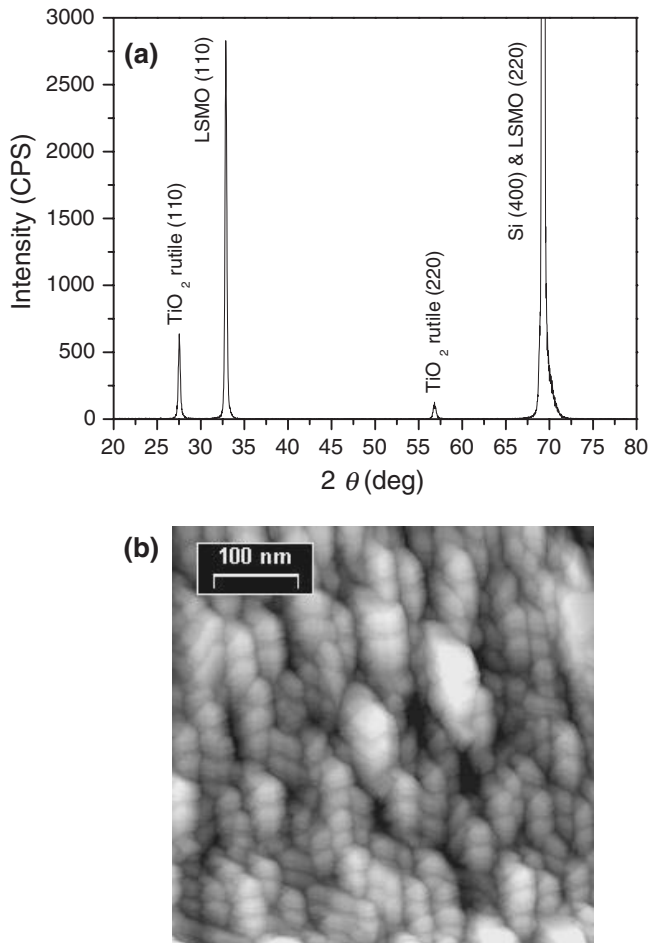


Fig. 1. XRD pattern (a) and STM image (b) of the (110)-oriented  $\text{La}_{2/3}\text{Sr}_{1/3}\text{MnO}_3$  (LSMO) thin films grown on  $\text{TiO}_2$ -buffered Si (100).

oriented. The full widths at half maximum of the (110) peaks of LSMO and  $\text{TiO}_2$  are about  $0.25^\circ$  and  $0.28^\circ$ , respectively, indicating excellent crystallinity. Moreover, the distances of the (110) lattice planes ( $d_{(110)}$ ), calculated from the XRD data, of the as-grown  $\text{TiO}_2$  rutile and LSMO films are about 3.237 Å and 2.721 Å. The lattice constants of the bulk  $\text{TiO}_2$  rutile are  $a = b \sim 4.594$  Å,  $c \sim 2.959$  Å giving  $d_{(110)}$  of 3.248 Å. The bulk LSMO is nearly cubic with  $a \sim 3.876$  Å and  $d_{(110)} \sim 2.741$  Å, respectively. The difference between the  $d_{(110)}$  of the as-grown LSMO films and bulk values possibly results from the tensile strain induced by the film-substrate lattice mismatch. The surface image of the LSMO film is shown in Fig. 1(b). The grain size is about 25 nm. Moreover, it is clear that the grains orient in the same in-plane direction.

The temperature dependence of resistivity,  $\rho(T)$ , as plotted in Fig. 2, indicates a clear I-M transition at 360 K and 376 K for a zero field and 5 T applied field, respectively. The MR, as defined by  $[\rho(H = 5\text{T}) - \rho(H = 0)]/\rho(H = 0)$ , is about  $-23\%$  around 350 K. It is worth noting that a large MR of about  $-20\%$  can be sustained even below 30 K.

The temperature dependence of the in-plane magnetization,  $M(T)$ , indicates that the as-grown film is ferromagnetic below 350 K, as presented in Fig. 3. Due to the limitation of our PPMS system, the  $M(T)$  can only be measured up to 350 K. By extrapolating the  $M(T)$  curve, the ferromagnetic  $T_C$  was estimated to be about 360 K. The inset of Fig. 3

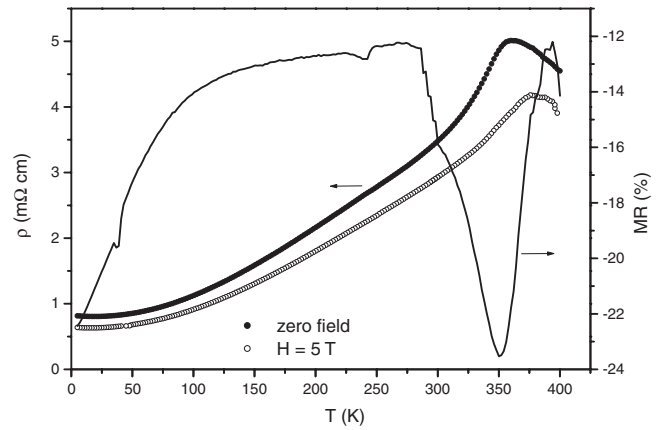


Fig. 2. Temperature dependence of the resistivity measured at magnetic fields of 0 and 5 T. The magnetoresistance (MR) defined as  $[\rho(H = 5\text{T}) - \rho(H = 0)]/\rho(H = 0)$  is also presented.

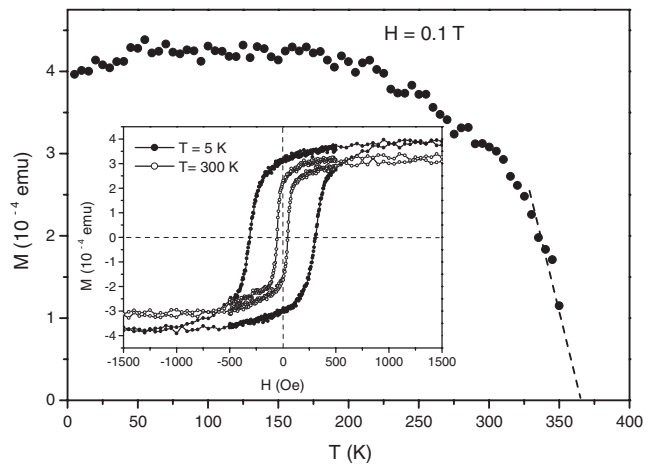


Fig. 3. Temperature dependence of magnetization measured in a magnetic field of 0.1 T applied along the plane of the film. The inset shows the magnetic hysteresis loop measured at 5 K and 300 K.

shows the field-dependent magnetization,  $M(H)$ , measured at 5 K and 300 K. The in-plane coercive fields are 60 Oe and 300 Oe at 300 K and 5 K, respectively. The values are larger than those of the  $c$ -axis-oriented films grown on  $\text{LaAlO}_3$  (LAO) substrates.<sup>2)</sup>

Figure 4(a) shows the normalized field-dependent resistance curves,  $R(H)/R(H_c)$ , where  $R(H_c)$  is the resistance measured at the coercive field of the correspondent temperature. The  $R(H)/R(H_c)$  at 300 K decreases almost linearly with increasing magnetic field up to 5 T. Nevertheless, the situation at 5 K is quite different. In this case, the  $R(H)/R(H_c)$  drops precipitously at low fields (0–0.2 T). As the applied magnetic field exceeds 0.5 T, the resistance becomes linear in the magnetic field again. The correlation between the  $M(H)$  and low-field  $R(H)/R(H_c)$  at 5 K is shown in Fig. 4(b). It is worth noting that the peaks of the  $R(H)/R(H_c)$  curves are closely associated with the coercive field. The resistivity and coercive fields of films grown in this work are much higher than those of epitaxial films grown on single-crystalline LAO substrates.<sup>2,15)</sup> Moreover, the large MR at low temperatures observed in these (110)-oriented LSMO films is absent in high-quality epitaxial films

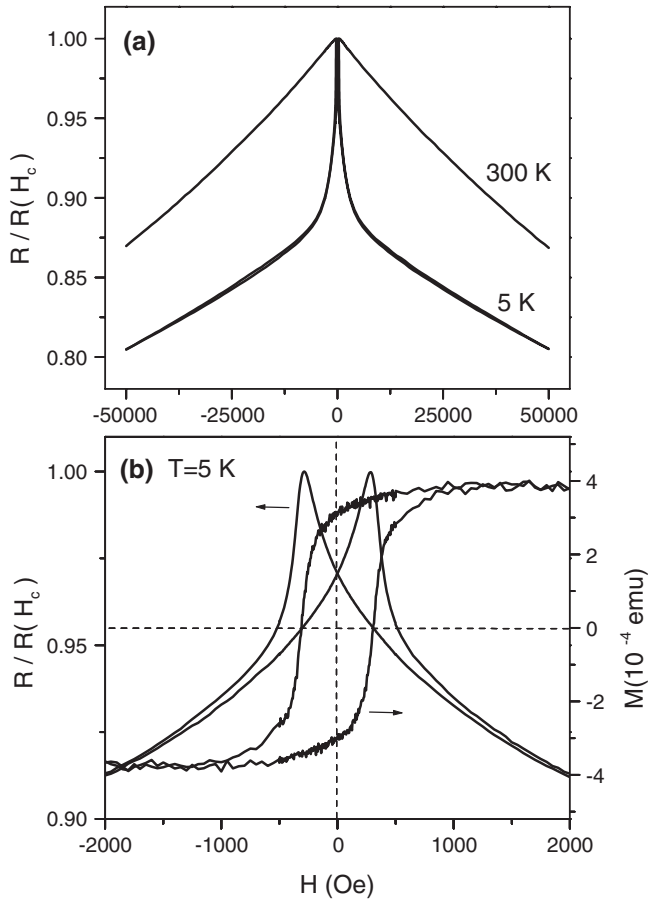


Fig. 4. (a) Normalized resistance,  $R/R(H_c)$ , as a function of in-plane magnetic fields measured at 300 K and 5 K. (b) The  $R/R(H_c)$  curve and the magnetization hysteresis loop measured at 5 K are plotted. The peaks of the  $R/R(H_c)$  curves are associated with the coercive fields.

grown on LAO. It is noted that similar results have been found in the “engineered” polycrystalline LCMO films<sup>16,17</sup> and attributed to the grain-boundary (GB) effects. The GB effects can result in the large MR at low temperatures and increase the resistivity and coercive field, without reducing the  $T_{IM}$ . For these films grown in this work, the higher resistivity can be ascribed to the spin-dependent scattering occurring in grain boundaries with magnetic inhomogeneity. The higher coercive field, on the other hand, may be due to the random orientation of magnetic domains possibly defined by the grains. As a result, the magnetic field needed to flip the magnetization of the whole domain is higher than that needed to propagate a domain.

Lastly, the large MR at low temperatures was attributed to the suppression of spin-dependent scattering by the applied fields. The coincidence of the  $R(H)/R(H_c)$  peaks with the coercive fields in the magnetization hysteresis loop indicates that spin-dependent scattering is dominant in the transport properties of as-grown films at low temperatures. The temperature dependence of the resistivity of manganite films also represents a much discussed issue of half-metallic material. In conventional ferromagnets, such as Fe, Co and Ni, a  $T^2$  dependence of resistivity, arising from the one-magnon scattering, is usually observed at low temperatures. However, the one-magnon scattering, which is a spin-flip scattering process, is theoretically forbidden in a perfect half

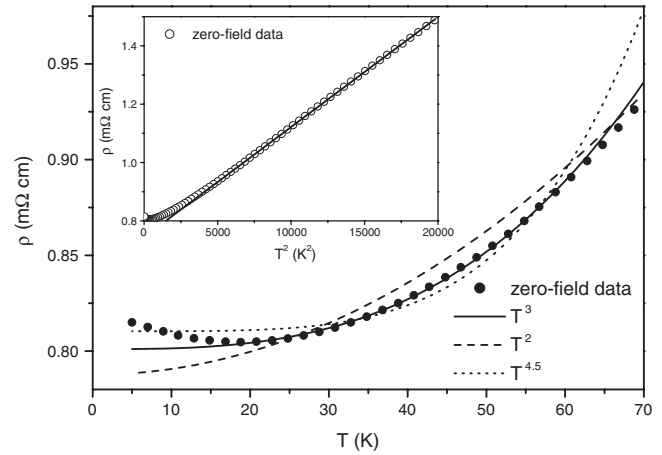


Fig. 5.  $\rho(T) = \rho_0 + AT^\alpha$  ( $\alpha = 2, 3$  and  $4.5$ ) fitting of resistivity. The  $T^2$  dependence of resistivity is also shown in the inset. A  $T^2$ - to  $T^3$ -dependence crossover is observed around 60 K. The semiconductive behavior below 20 K can be attributed to the grain-boundary resistance.

metal due to the absence of minority spin states. Based on the rigid-band picture, Kubo and Ohata<sup>18</sup>) have proposed that two-magnon scattering, which gives a  $T^{4.5}$  dependence of resistivity, is dominant at low temperatures. On the other hand, a  $T^3$  dependence has been proposed by Furukawa<sup>19</sup>) who considered an unconventional one-magnon scattering due to spin-fluctuation-induced non-rigid minority band at finite temperatures. The inset of Fig. 5 shows the  $T^2$  plot of the resistivity of the as-grown LSMO film. The resistivity fits well with  $\rho(T) = \rho_0 + AT^2$  between 144 K and 60 K. However, it deviates from the  $T^2$  behavior significantly for  $T < 60$  K. For comparison, we show in Fig. 5 the fitting of  $\rho(T) = \rho_0 + AT^\alpha$  with  $\alpha = 2, 3$  and  $4.5$  below 70 K. It is clear that the resistivity is best fitted by  $\rho(T) = \rho_0 + AT^3$  between 60 K and 20 K. The  $T^2$ - to  $T^3$ -dependence crossover at around 60 K, though slightly higher, is in good agreement with the theoretical prediction.<sup>19</sup>) The slightly higher crossover temperature may have arisen from the enhanced incoherence of the minority band due to grain boundaries. The semiconductive behavior below 20 K can also be attributed to the GB resistance.

In summary, we have deposited  $\text{La}_{2/3}\text{Sr}_{1/3}\text{MnO}_3$  thin films on Si substrates by means of a  $\text{TiO}_2$  buffer layer. The as-grown films were pure (110)-oriented and exhibited both insulator-metal and ferromagnetic transitions at about 360 K, which is comparable to the bulk value. Moreover, a large MR ( $\Delta\rho/\rho(H=0) \sim -20\%$ ) in a magnetic field of 5 T was observed not only around  $T_{IM}$  but also below 30 K. The coincidence of the peaks of field-dependent MR loop with the coercive field at 5 K indicates that spin-dependent scattering occurring in the grain boundaries may have played an important role in the low-temperature magneto-transport properties of these (110)-oriented LSMO films. The temperature dependence of resistivity displayed a  $T^2$ - to  $T^3$ -dependence crossover at around 60 K. This temperature is in fair agreement with the theoretically estimated value of 50 K based on the unconventional one-magnon scattering mechanism.

This work was supported by the National Science Council of Taiwan, R.O.C. under Grant Nos: NSC90-2112-M-009-025 and NSC90-2112-M-009-030.

- 1) J.-H. Park, E. Vescovo, H.-J. Kim, C. Kwon, R. Ramesh and T. Venkatesan: *Nature* **392** (1998) 794.
- 2) B. Nadgorny, I. I. Mazin, M. Osofsky, R. J. Soulen, Jr., P. Broussard, R. M. Stroud, D. J. Singh, V. G. Harris, A. Arsenov and Y. Mukovskii: *Phys. Rev. B* **63** (2001) 184433.
- 3) G. A. Prinz: *Phys. Today* **48** (1995) 58.
- 4) G. A. Prinz: *Science* **282** (1998) 1660.
- 5) G. Srinivasan, V. S. Babu and M. S. Seehra: *Appl. Phys. Lett.* **67** (1995) 2090.
- 6) W. Zhang, I. W. Boyd, M. Elliott and W. Herrenden-Harkerand: *Appl. Phys. Lett.* **69** (1996) 1154.
- 7) P. J. Kung, D. B. Fenner, D. M. Potrepka and J. I. Budick: *Appl. Phys. Lett.* **69** (1996) 427.
- 8) E. S. Vlahov, K. Dorr, K.-H. Muller, K. A. Nenkov, A. Handstein, T. I. Donchev, A. Y. Spasov and G. D. Beshkov: *Vacuum* **58** (2000) 364.
- 9) K. H. Wang and Y. S. Leung: *Thin Solid Films* **354** (1999) 55.
- 10) D. Kumar, S. Chattopadhyay, W. M. Gilmore, C. B. Lee, J. Sankar, A. Kvit, A. K. Sharma, J. Narayan, S. V. Pietambaram and R. K. Singh: *Appl. Phys. Lett.* **78** (2001) 1098.
- 11) W. Zhang, X. Wang and I. W. Boyd: *Appl. Surf. Sci.* **138-139** (1999) 563.
- 12) Z. Trajanovic, C. Kwon, M. C. Robson, K.-C. Kim, M. Rajeswari, R. Ramesh, T. Venkatesan, S. E. Lofland, S. M. Bhagat and D. Fork: *Appl. Phys. Lett.* **69** (1996) 1005.
- 13) S. J. Liu, J. Y. Juang, K. H. Wu, T. M. Uen, Y. S. Gou and J.-Y. Lin: *Appl. Phys. Lett.* **80** (2002) 4202.
- 14) P. I. Lin, C. W. Liu, C. C. Hsieh, K. H. Wu, J. Y. Juang, T. M. Uen, Y. S. Gou and J.-Y. Lin: *Jpn. J. Appl. Phys.* **40** (2001) L377.
- 15) J. C. Chen, S. C. Law, L. C. Tung, C. C. Chi and W. Guan: *Phys. Rev. B* **60** (1999) 12143.
- 16) A. Gupta, G. Q. Gong, G. Xiao, P. R. Duncombe, P. Lecoeur, P. Trouilloud, Y. Y. Wang, V. P. Dravid and J. Z. Sun: *Phys. Rev. B* **54** (1996) R15629.
- 17) X. W. Li, A. Gupta, G. Xiao and G. Q. Gong: *Appl. Phys. Lett.* **71** (1997) 1124.
- 18) K. Kubo and N. Ohata: *J. Phys. Soc. Jpn.* **33** (1972) 21.
- 19) N. Furukawa: *J. Phys. Soc. Jpn.* **69** (2000) 1954.